JACS
JOURNAL OF THE AMERICAN CHEMICAL SOCIETY

Communication

pubs.acs.org/JACS

Remote Sensing by Plasmonic Transport

Seung Joon Lee and Martin Moskovits*

Department of Chemistry and Biochemistry, University of California, Santa Barbara, California 93106-9510, United States

Supporting Information

ABSTRACT: Arrays of periodically disposed silver nanowires embedded in alumina were shown to be capable of conducting plasmons excited by laser illuminating one end of the array to its opposite end where surface-enhanced Raman of molecules resident among the tips of the nanowires was excited. The SERS signals, in turn, excited plasmons which propagated back to the originally illuminated ends of the nanowires where they emitted light signals that were collected and spectroscopically dispersed, in essence creating a sensor capable of exciting and collecting SERS remotely. For nanowire arrays with interwire gaps of ~11 nm and lengths of ~3.3 μm (i.e., after a ~6.6 μm round trip) the SERS signals obtained by remote sensing were rather strong, ~5% the intensity of those obtained by exciting the molecules resident among the nanowire tips directly.

Plasmonic transport along nanowires (NWs) is an actively studied phenomenon.[1−10] First reported by Dickson and Lyon in 2000 the conversion of light illuminating the end of a noble metal NW into surface plasmons which then couples out as light at the distal end of the NW has now been described by several workers who have reported, among other phenomena, the preservation of coherence between the exciting light and the propagating plasmon.[11] Moreover, it is now known that, in addition to the ends of the NWs, other structural features along the NW can act as antennae coupling the energy of the plasmon out as light.[4] For example, nanoparticles (NPs) sessile upon the NW at some intermediate point along its length can couple light out; and, if molecules exist in the gap between the NW and the NP, SERS can be excited from those NW-NP junctions even when the NW is illuminated only at one of its ends which might be several micrometers removed from those junctions.[6,7] The mechanism of plasmonic conductance in NWs is in some ways isomorphic with the dynamics of energy flow in a linear array of equivalent oscillators compressed at one end. Just as that compression can be written as a coherent superposition of the normal modes of the linear array which (in the absence of anharmonicities and energy-loss terms) will correspond to an excitation that travels back and forth along the linear array, so the illumination of a NW at one end excites a superposition of many of its plasmonic normal modes, with the electron-density bolus traveling back and forth and reflecting off its ends. Of course, the plasmonic amplitude is attenuated as it propagates along the NW, largely as a result of electrical resistance. Plasmonic conductance is exponentially attenuated as a function of the length of the NW with attenuation constants of ~2 to ~4 μm.[3,7]

In this communication we report a probe that can detect by SERS molecules which are situated at the distal end of a silver NW bundle such that both the excitation fields and the SERS signals are propagated plasmonically by the NW bundle, as shown schematically in Figure 1. This approach allows, for example, SERS to be detected from species interacting with the end of a gold or silver NW probe (most likely composed of a bundle of NWs for increased signal collection ability) attached to the end of an optical fiber and introduced into a liquid, or, by a catheter, into tissue or a blood vessel.

The construction of this "plasmon probe" is described in detail in the Supporting Information. Briefly, it consists of an array of silver NWs deposited electrochemically in a highly ordered porous anodic alumina (PAO) template whose pores were widened in phosphoric acid to achieve the desired pore-to-pore gap, or, more generally, the optimal combination of interwire gap distance and NW diameter, which will produce the largest signals at the excitation wavelength used. (The center-to-center distance between pores in our samples is 100 nm. As pore-widening proceeds, the pore-wall thickness decreases which eventually translates into an array of thicker NWs with smaller interwire gaps.[12]) The small inter-NW gaps are essential since, for light polarized across the lengths of the NWs, they constitute the hot spots in which the largest signals will ordinarily be excited. Two sets of samples were prepared in templates, respectively, with 11 and 33 nm interwire gap distances (corresponding to 88 and 68 nm NW diameters, respectively). For each of the two classes of sample, probes with NW lengths ranging from less than 1 μm to over 3 μm were fabricated to gauge the signal attenuation properties.

After depositing silver into its pores the anodic oxide templates were mounted on precleaned glass cover slides (with the open side of the pores against the slide) using index matching adhesive (NOA 61, Norland Product, n = 1.56) to reduce reflection at the interface, and the aluminum on the backside of PAO templates was removed by etching in saturated aqueous mercury chloride solution. The alumina matrix of the templates was then partially etched in 0.1 M aqueous NaOH solution to expose the NW tips; the etching time for the tip exposure was chosen following a set of experiments in which templates were etched for a variable time from 120 to 360 s in 30 s intervals and then imaged by SEM. The exposed tips were functionalized with a Raman reporter molecule by dipping the templates in 0.5 mM ethanolic 4-aminobenzenethiol (ABT) solution.

The resulting "plasmon probe", which is shown schematically in Figure 1, was used to measure the SERS intensity using

Received: May 14, 2012
Published: July 2, 2012

   dx.doi.org/10.1021/ja3046662 | J. Am. Chem. Soc. 2012, 134, 11384−11387

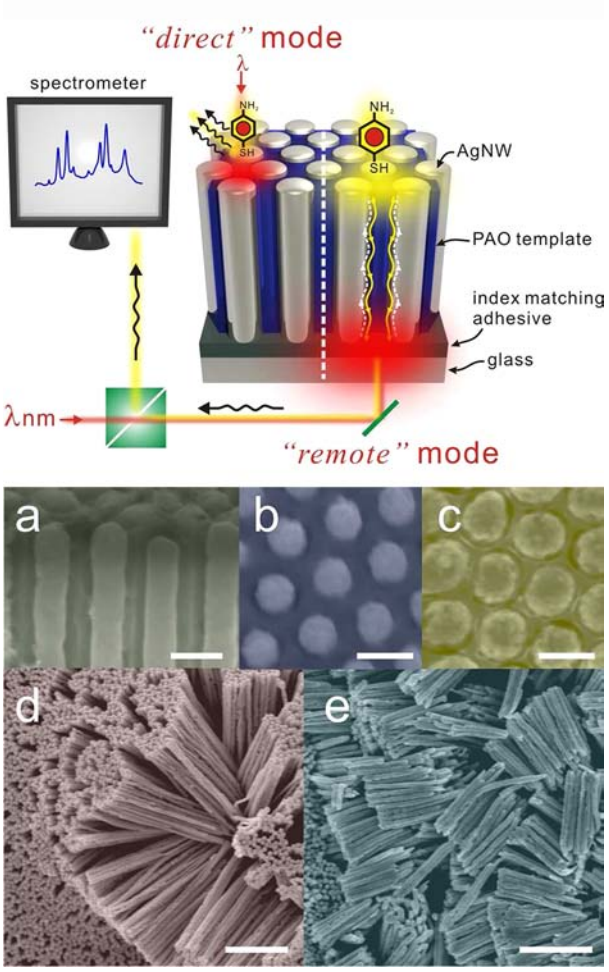

Figure 1. (Top) Schematic of the SERS sensor by remote plasmon conduction system. (Bottom) SEM images of the silver nanowire bundles comprising the sensor; (a) cross-sectional view for a probe with gap of ~33 nm showing the nanowires embedded in anodic alumina but with their tips slightly exposed to accommodate the analyte; (b, c) top views for samples with interwire gaps of, respectively, ~33 and ~11 nm, after tip exposure out of PAO templates. (d, e) AgNW bundles with ~2.2 μm length (~33 nm gap) and ~1 μm length (~11 nm gap) after release from the PAO template by etching the alumina matrix. Scale bar: (a, b, and c) 100 nm and (d and e) 1 μm.

probes with varying NW lengths and NW-to-NW gap distance both by illuminating the sample at, and collecting the SERS signals from, the end of the NW at which the adsorbate (ABT) is located (*direct* excitation mode), or by illuminating the end of the NW remote from the end at which the adsorbate resides, and measuring the SERS signals that had traveled back to the end illuminated by the excitation laser, presumably by the intermediacy of plasmonic transport (*remote* excitation mode). A collection of SEM images for samples is shown in Figure 1.

Excellent SERS spectra of the adsorbate were obtained by both *direct* and *remote* excitation modes (Figure 2). That such high SERS intensities were obtained by *remote* excitation suggests that in this mode the exciting laser launched surface plasmons in the silver NW bundles which reached the remote end of the NW where the adsorbate resides; some of the plasmon energy coupled out at that point to create an optical near field in the inter-NW gaps at the remote end which excited the adsorbate. The Raman shifted (as well as the elastically

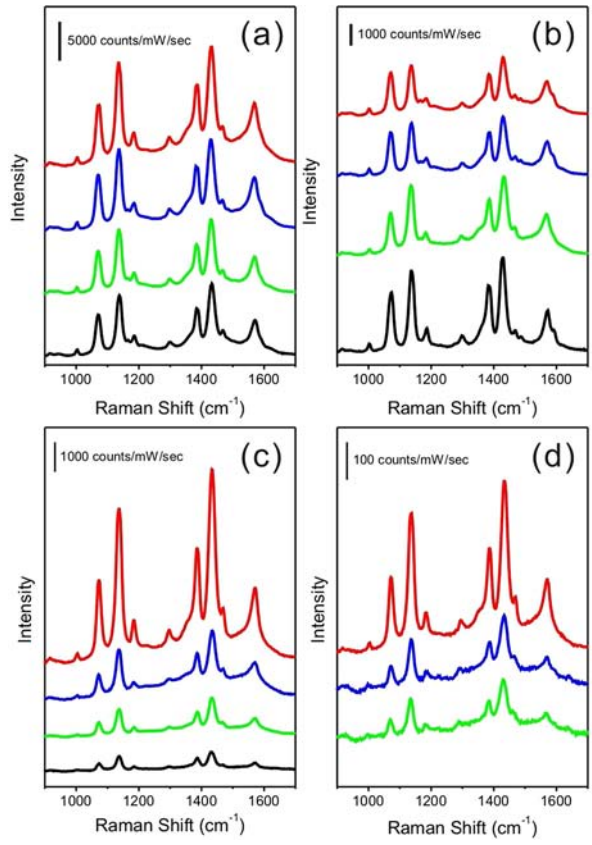

Figure 2. Averaged SERS spectra taken by *direct* excitation (a and b) and *remote* excitation (c and d); (a and c) Gap of ~11 nm with NW length of ~920 nm (red), ~1960 nm (blue), ~2520 nm (green), and ~3300 nm (black), respectively. (b and d) Gap of ~33 nm with NW length of ~860 nm (red), ~1880 nm (blue), ~2160 nm (green), and ~2880 nm (black), respectively. Negligibly low SERS signals were observed for the sample with ~33 nm gap and ~2880 nm NW length.

scattered) light then excites plasmons in the NWs which traveled back down the NW ultimately coupling out as radiation from the end of the NW originally excited, which is collected and dispersed in a spectrometer.

The SERS data are summarized in Table 1. The arrays with 88 nm diameter NWs, i.e. arrays with the smaller (11 nm)

Table 1. Results of SERS Measurements

Gap: 11 ± 4 nm (NW diameter: 88 ± 4 nm)[a]		
NW length	Tip[b]	Remote[c]
920 ± 130 nm	8227 ± 2683	3432 ± 629
1960 ± 100 nm	7293 ± 342	979 ± 263
2520 ± 295 nm	5267 ± 148	575 ± 135
3300 ± 200 nm	6047 ± 804	302 ± 87
Gap: 33 ± 6 nm (NW Diameter: 68 ± 7 nm)[a]		
NW length	Tip[b]	Remote[c]
860 ± 120 nm	1842 ± 339	123 ± 26
1880 ± 150 nm	1897 ± 396	31 ± 9
2160 ± 150 nm	1958 ± 289	13 ± 5
2880 ± 195 nm	2484 ± 1234	Not observed

[a]Counts/mW/s; SERS intensities were taken by subtracting background intensity at 1020 cm^{-1} from the peak at 1070 cm^{-1}. [b]Obtained by exciting the ABT-capped end of the NW (*direct* excitation). [c]Obtained by exciting the uncapped end of NW (*remote* excitation).

dx.doi.org/10.1021/ja3046662 | J. Am. Chem. Soc. 2012, 134, 11384–11387

interwire gap, produced significantly more intense SERS signals by *remote* excitation than did the array of 68 nm diameter NWs with the larger (33 nm) interwire gap. We show below that this is due to both the fact that bundles of larger diameter NWs excited more intense SERS (as shown by the *direct* excitation results), likely because the narrower gaps functioned as better SERS hot spots, and the fact that the plasmonic transport through the bundle of the larger diameter NWs was less attenuated than in the bundle of the smaller diameter NWs.

The SERS intensity data as a function of NW lengths are plotted in Figure 3a. The data are presented as the logarithm of the intensities to enable the large range of intensity values involved to be accommodated in a single figure. It is at once clear that the SERS data measured by *direct* excitation are approximately independent of the NW lengths, whereas the data measured by *remote* excitation are exponentially dependent on the NW lengths. The small variation in intensities observed with *direct* excitation is likely dominated by sample-to-sample variability. Measurements as a function of NW length were done on separate samples for each length. That the SERS intensity values (in *direct* excitation) varied by less than a factor of 1.5 for so large an ensemble of samples fabricated using so many steps is an indication of the high level of sample-to-sample reproducibility. (For completeness one should state in passing that for short NWs it is not unlikely that the SERS intensity would also be somewhat NW length dependent, even in the *direct* excitation mode, since the fields in the hot spots in the gaps between the NWs would in that case be affected by the NW length. However, this is not expected to be a large effect.)

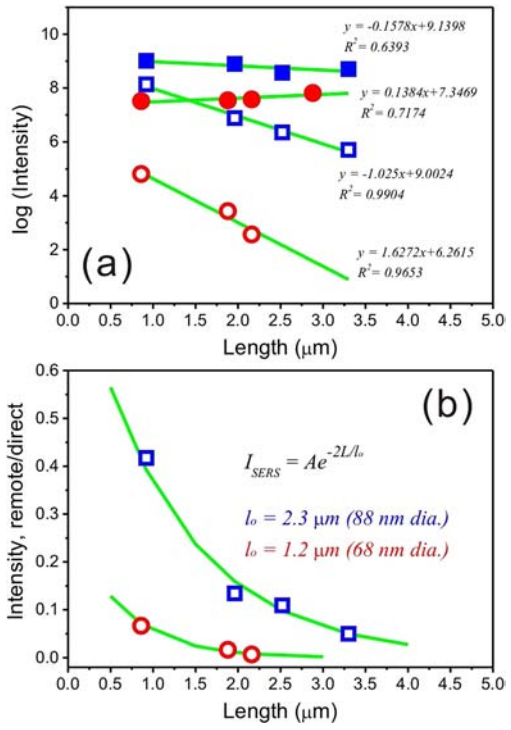

Figure 3. (a) Log_{10} SERS intensities as a function of NW lengths taken by *direct* (filled symbols) and *remote* (open symbols) excitation of samples with 88 nm NW diameter (squares) and 68 nm NW diameter (circles), respectively. (b) Normalized SERS intensities (*remote*/*direct*) as a function of NW lengths with 88 nm NW diameter (open square) and 68 nm NW diameter (open circle) (green lines are best-fit curves).

The SERS intensity measured by *direct* excitation is on average smaller by a factor of ~3 for the sample with the larger inter-NW gap (and the smaller NW diameter) than that measured for the samples with the smaller inter-NW gap. One can also dismiss the possibility that the *remote* SERS signal arises from light (as opposed to plasmons) transmission through the sample, ultimately exciting SERS at the distal end of the array. UV−visible transmission spectroscopy carried out on the samples used in this study (see Supporting Information) shows that even for the arrays with the shortest nanowires the maximum optical transmission in the pertinent wavelength range is <1%, and <0.1% for the arrays with the longest nanowires, totally excluding optical transmission as a significant contributor to the excitation of the *remote* SERS signals.

Dividing the SERS intensity of the Raman band at 1070 cm^{-1} measured by *remote* excitation by corresponding values obtained by *direct* excitation in order to factor out common factors affecting the intensity measurements, and also to factor out the effect of the larger overall SERS cross section for molecules adsorbed in the gaps between the larger diameter NWs, and plotting the data as a function of NW length, L, (Figure 3b) one finds that the data fit an expression of the following form:

$$I_{SERS} = A \cdot \exp(-2L/l_o) \quad (1)$$

The values of l_o were found to be 2.3 and 1.2 μm, respectively, for the bundles of 88 nm diameter and 68 nm diameter NWs.

The factor 2 in the exponential of eq 1 arises from the fact that the SERS signal was measured after a plasmonic round-trip in the NW, and the prefactor A includes all of the appropriate contributions such as the coupling of the incident and Raman scattered fields into the respective ends of the NW thereby launching plasmons, and the out-coupling of the plasmons into optical near fields out of the two ends. (However, it would not include the contribution from the effective SERS enhancement since this factor is canceled out by scaling the *remote* excitation data with those measured by *direct* excitation.) The prefactor would also include the effect of the larger metal cross-sectional area presented to the incoming optical fields by the 88 nm diameter NWs as compared to the 68 nm diameter NWs. The metal area fractions of the hexagonally arranged bundles of NWs are, respectively, 0.7 and 0.42 for the 88 and 68 nm diameter NW bundles.

The 1.9-fold increase in the values of l_o on going from the 88 nm diameter to the 68 nm diameter nanowire bundle is most likely due to the greater electrical resistance of the narrower nanowire. The inverse of l_o is essentially a measure of the ohmic loss per unit nanowire length; the ratio of the two values of l_o should therefore scale as the ratio of the cross-sectional areas of the nanowires. That area ratio is equal to $(44)^2/(34)^2 = 1.7$, in rather close agreement with the measured ratio (1.9) of the two l_o values.

The ratio of the prefactors, A, computed for the two sets of NW sensors is $A_{88}/A_{68} \approx 2.9$. If all factors affecting the prefactor A had been common to the two sets of NWs with the exception of the metal area fraction, then one would have expected a prefactor ratio of ~0.7/0.42 = 1.7. The larger measured prefactor ratio implies that some other components of the prefactor, such as the efficiency of plasmon-photon coupling at the ends of the NWs, are also greater for the bundle of the more closely spaced and broader NWs.

dx.doi.org/10.1021/ja3046662 | J. Am. Chem. Soc. 2012, 134, 11384−11387

■ ASSOCIATED CONTENT

Supporting Information

Materials and methods, experimental details, and control experiments. This material is available free of charge via the Internet at http://pubs.acs.org.

■ AUTHOR INFORMATION

Corresponding Author

moskovits@chem.ucsb.edu

Notes

The authors declare no competing financial interest.

■ ACKNOWLEDGMENTS

We gratefully acknowledge support from the Institute for Collaborative Biotechnologies through Grant DAAD19-03-D-0004 from the U.S. Army Research Office. We also made extensive use of the MRL Central Facilities at UCSB supported by the National Science Foundation under Award Nos. DMR-0080034 and DMR-0216466 for the HRTEM/STEM microscopy.

■ REFERENCES

(1) Dickson, R. M.; Lyon, L. A. *J. Phys. Chem. B* **2000**, *104*, 6095−6098.
(2) Akimov, A. V.; Mukherjee, A.; Yu, C. L.; Chang, D. E.; Zibrov, A. S.; Hemmer, P. R.; Park, H.; Lukin, M. D. *Nature* **2007**, *450*, 402−406.
(3) Sanders, A. W.; Routenberg, D. A.; Wiley, B. J.; Xia, Y.; Dufresne, E. R.; Reed, M. A. *Nano Lett.* **2006**, *6*, 1822−1826.
(4) Knight, M. W.; Grady, N. K.; Bardhan, R.; Hao, F.; Nordlander, P.; Halas, N. *Nano Lett.* **2007**, *7*, 2346−2350.
(5) Fang, Z.; Fan, L.; Lin, C.; Zhang, D.; Meixner, A. J.; Zhu, X. *Nano Lett.* **2011**, *11*, 1676−1680.
(6) Fang, Y.; Wei, H.; Hao, F.; Nordlander, P.; Xu, H. *Nano Lett.* **2009**, *9*, 2049−2053.
(7) Hutchison, J. A.; Centeno, S. P.; Odaka, H.; Fukumura, H.; Hofkens, J.; Uji-I, H. *Nano Lett.* **2009**, *9*, 995−1001.
(8) Ditlbacher, H.; Hohenau, A.; Wagner, D.; Kreibig, U.; Rogers, M.; Hofer, F.; Aussenegg, F. R.; Krenn, J. R. *Phys. Rev. Lett.* **2005**, *95*, 257403.
(9) Rewitz, C.; Keitzl, T.; Tuchscherer, P.; Huang, J.-S.; Geisler, P.; Razinskas, G.; Hecht, B.; Brixner, T. *Nano Lett.* **2012**, *12* (1), 45−49.
(10) Li, Z.; Bao, K.; Fang, Y.; Huang, Y.; Nordlander, P.; Xu, H. *Nano Lett.* **2010**, *10*, 1831−1835.
(11) Kolesov, R.; Grotz, B.; Balasubramanian, G.; Stöhr, J.; Nicolet, A. A. L.; Hemmer, P. R.; Jelezko, F.; Wrachtrup, J. *Nat. Phys.* **2009**, *5*, 470−474.
(12) Lee, S. J.; Guan, Z.; Xu, H.; Moskovits, M. *J. Phys. Chem. C* **2007**, *111*, 17985−17988.